

## Dispersion of a Hole in a Two-Dimensional $\text{Cu}_3\text{O}_4$ Plane: A Tale of Two Singlets

Mark S. Golden, Heike C. Schmelz, Martin Knupfer, Stefan Haffner, Gernot Krabbes, and Jörg Fink  
*Institute for Solid State and Materials Research (IFW) Dresden, P.O. Box 270016, D-01171 Dresden, Germany*

Victor Yu. Yushankhai,\* Helge Rosner, and Roland Hayn  
*Max Planck Arbeitsgruppe "Elektronensysteme," Technische Universität Dresden, D-01062 Dresden, Germany*

Andreas Müller  
*Institut für Physik, Humboldt Universität zu Berlin, Invalidenstrasse 110, D-10115, Berlin, Germany*

Gerd Reichardt  
*BESSY GmbH, Lentzallee 100, D-14195 Berlin, Germany*  
 (Received 3 February 1997)

Polarization-dependent angle-resolved photoemission spectroscopy measurements of  $\text{Ba}_2\text{Cu}_3\text{O}_4\text{Cl}_2$  indicate the presence of two different Zhang-Rice singlets in the two-dimensional  $\text{Cu}_3\text{O}_4$  plane of this insulating copper oxychloride. With the aid of model calculations, we show that one singlet is moving in the antiferromagnetically ordered cupratelike  $\text{Cu}_A\text{O}_2$  subsystem and the other on the effectively paramagnetic sublattice formed by the extra  $\text{Cu}_B$  atoms. The dispersion of the former is thus determined by the superexchange integral  $J_A$ , and that of the latter by the hopping integral  $t_B$ . Consequently, as far as the role of the magnetic background is concerned, the dispersion relation of a single hole in this system represents simultaneously both the low and very high doping limits of a cuprate plane in a single structure. [S0031-9007(97)03226-2]

PACS numbers: 74.25.Jb, 71.27.+a, 79.60.Bm

The electronic structure of the  $\text{CuO}_2$  planes is believed to hold the key to high temperature superconductivity in the cuprates. The lowest electron removal state in the  $\text{CuO}_2$  plane cuprates is the so-called Zhang-Rice singlet (ZRS) [1], in which the spin of an intrinsic copper hole, located in the  $\text{Cu } 3d_{x^2-y^2}$  orbital, is compensated by the spin of a hole distributed over the  $2p_{x,y}$  orbitals of the surrounding four oxygen atoms. The ZRS forms as a result of  $p$ -type doping or of electron removal in photoemission spectroscopy. Recently, angle-resolved photoemission spectroscopy (ARPES) studies of the dispersion of a ZRS in the undoped  $\text{CuO}_2$  plane of the oxychloride  $\text{Sr}_2\text{CuO}_2\text{Cl}_2$  have caused considerable interest [2,3], as these data were in approximate agreement with the earlier predictions of the  $t$ - $J$  model [4].

In this Letter, we present a combined experimental and theoretical study of the dispersion of a single hole in the two-dimensional  $\text{Cu}_3\text{O}_4$  plane of  $\text{Ba}_2\text{Cu}_3\text{O}_4\text{Cl}_2$ . This plane can be regarded as a cupratelike  $\text{Cu}_A\text{O}_2$  subsystem with additional copper atoms, denoted here as  $\text{Cu}_B$ . Both  $\text{Cu}_A$  and  $\text{Cu}_B$  order antiferromagnetically: the former at 330 K and the latter at only 31 K [5]. We show that as a consequence of this, in a single ARPES experiment carried out at  $T = 360$  K, it is possible to study the dispersion of a ZRS in both an antiferromagnetic and paramagnetic spin background simultaneously in the same  $\text{Cu}_3\text{O}_4$  plane.

$\text{Ba}_2\text{Cu}_3\text{O}_4\text{Cl}_2$  is a tetragonal insulator, with  $a = 5.517$  and  $c = 13.808$  Å [6]. The  $\text{Cu}_3\text{O}_4$  planes are highly two dimensional and are separated by ionic Ba-Cl block layers.

The superposition of the  $\text{Cu}_B$  atoms on the  $\text{Cu}_A\text{O}_2$  sublattice to give the overall  $\text{Cu}_3\text{O}_4$  stoichiometry is sketched in Fig. 1, as is one of the mirror planes of the  $\text{Cu}_3\text{O}_4$  surface, labeled  $M_1$ . The same  $\text{Cu}_3\text{O}_4$  plane geometry is found in  $\text{Sr}_2\text{Cu}_3\text{O}_4\text{Cl}_2$ , in which a ferromagnetic moment due to pseudodipolar coupling between the two copper lattices was recently observed [7]. Single crystals of  $\text{Ba}_2\text{Cu}_3\text{O}_4\text{Cl}_2$  were grown from the melt, and were cleaved *in situ* for ARPES measurements recorded at the U2-FSGM beam line [8] at BESSY with a photon energy of 35 eV. The experimental resolution was set to 160 meV in energy and  $2^\circ$  in angle (corresponding to a  $\mathbf{k}$  resolution of  $0.16\pi/a$ ). During the measurements, the crystals were held at a temperature of 360 K, as this was found to prolong the life of the cleaved surface and reduce charging effects.

Figure 2 shows a series of ARPES spectra recorded along the  $(k_x, 0)$  direction in  $\mathbf{k}$  space, reaching beyond the edge of the second Brillouin zone (BZ). This direction is  $45^\circ$  to the Cu-O bonds in real space and is parallel to  $M_1$  in Fig. 1. The electric field vector of the synchrotron radiation was perpendicular to  $M_1$ . There are three main features observed in the energy range shown in Fig. 2, labeled A, B, and C. The deeper lying valence band features, B and C, are at least partially due to bands corresponding to the nonmixing oxygen states observed recently for  $\text{Sr}_2\text{CuO}_2\text{Cl}_2$  [3]. A detailed discussion of features B and C, as well as other details of the ARPES spectra, will form the subject of a forthcoming publication [9]. It is the behavior of the feature at lowest binding energies (BE) that

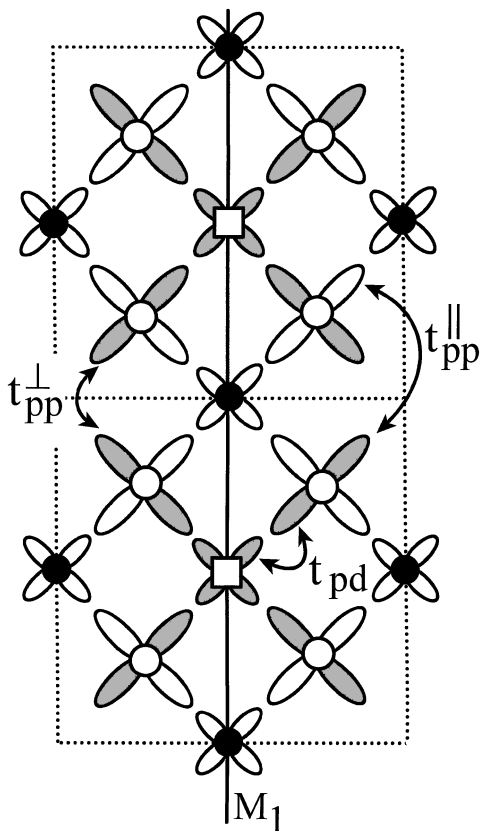


FIG. 1. Two unit cells of the  $\text{Cu}_3\text{O}_4$  plane of  $\text{Ba}_2\text{Cu}_3\text{O}_4\text{Cl}_2$  showing: ( $\bullet$ ) cupratelike  $\text{Cu}_A$ , ( $\square$ ) additional  $\text{Cu}_B$ , and ( $\circ$ ) oxygen. The  $\text{Cu } 3d_{x^2-y^2}$  and  $\text{O } 2p_{x,y}$  orbitals are also shown. The orbitals relevant for the motion of the ZRS on the  $\text{Cu}_B$  sublattice are shaded. Also shown schematically are the hopping matrix elements  $t_{pd}$ ,  $t_{pp}^{\parallel}$ , and  $t_{pp}^{\perp}$ , as well as a mirror plane of the  $\text{Cu}_3\text{O}_4$  surface, marked  $M_1$ .

prompted the present article. On moving away from the  $\Gamma$  point, a weak structure emerges from the main valence band and grows in intensity as its BE decreases, reaching a minimal BE of  $\sim 0.8$  eV at  $(\pi, 0)$ . At this  $\mathbf{k}$  value, the peak has a width of some 700 meV and displays a considerable asymmetry to the high BE side. Spectra recorded at  $(\pi, 0)$  under the same conditions, except with a total energy resolution of 70 meV, were identical.

At this stage it is instructive to compare these data with those observed for the  $\text{CuO}_2$  plane of  $\text{Sr}_2\text{CuO}_2\text{Cl}_2$ . The analogous ARPES spectra showed a similar feature increasing in intensity and dispersing to lower BE's, reaching both maximal intensity and minimal BE at the  $(\pi/2, \pi/2)$  point of the  $\text{Sr}_2\text{CuO}_2\text{Cl}_2$  BZ [2,3], which is equivalent to the  $(\pi, 0)$  point of the  $\text{Ba}_2\text{Cu}_3\text{O}_4\text{Cl}_2$  BZ. On going beyond  $(\pi/2, \pi/2)_{\text{Sr}}$ , the ZRS peak in  $\text{Sr}_2\text{CuO}_2\text{Cl}_2$  dispersed back to higher BE, and its spectral weight fell away very rapidly, thus resulting in a strongly asymmetric intensity profile as a function of  $\mathbf{k}$  around  $(\pi/2, \pi/2)_{\text{Sr}}$ .

As can be seen from Fig. 2, in  $\text{Ba}_2\text{Cu}_3\text{O}_4\text{Cl}_2$ , however, significant spectral weight remains at about 1 eV BE over a large region of  $\mathbf{k}$  space between  $(\pi, 0)$  and  $(3\pi, 0)$ . In

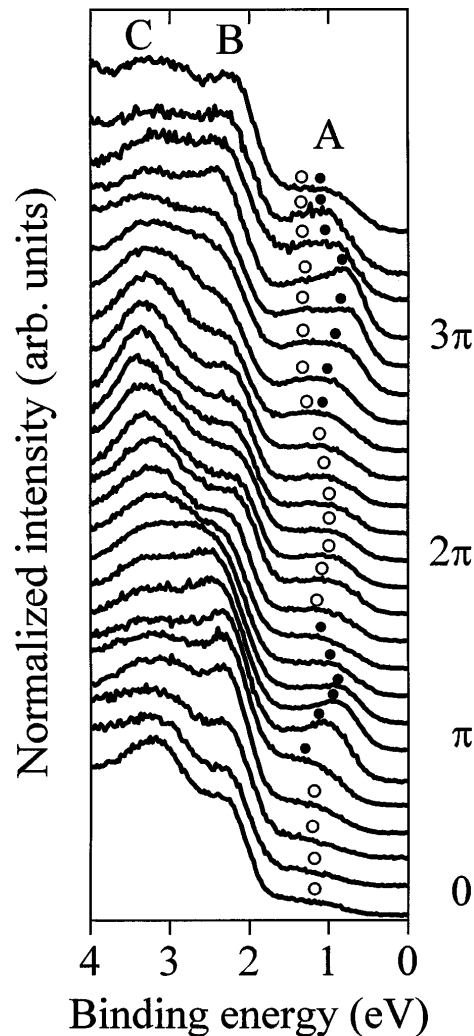


FIG. 2. ARPES spectra of  $\text{Ba}_2\text{Cu}_3\text{O}_4\text{Cl}_2$  measured along the  $(k_x, 0)$  direction. The values of  $k_x$  are expressed in terms of  $1/a$  ( $\text{\AA}^{-1}$ ). For the experimental details, see the text.

addition, approaching  $(3\pi, 0)$ , the line shape is strongly suggestive of the presence of two components (as marked in Fig. 2). Thus, while the dispersion of the lowest BE structure observed here near  $(\pi, 0)$  and  $(3\pi, 0)$  is similar to that in  $\text{Sr}_2\text{CuO}_2\text{Cl}_2$ , the existence of a clear structure remaining at about  $\sim 1$  eV between  $(\pi, 0)$  and  $(3\pi, 0)$  and the double-peaked nature of the feature in  $\text{Ba}_2\text{Cu}_3\text{O}_4\text{Cl}_2$  are significant and important differences with respect to the  $\text{CuO}_2$  plane oxychloride. We suggest that these differences indicate that the data shown in Fig. 1 can be interpreted in terms of two singlets  $\text{ZRS}_A$  and  $\text{ZRS}_B$ , where the  $3d_{x^2-y^2}$  orbitals of the  $\text{Cu}_A$  and  $\text{Cu}_B$  are hybridized with different subsystems of the in-plane  $\text{O } 2p_{x,y}$  orbitals (see Fig. 1). The filled and open circles in Fig. 2 represent the energy positions of  $\text{ZRS}_A$  and  $\text{ZRS}_B$ , respectively.

In Fig. 3, we provide indirect experimental evidence that the lowest lying electron removal states in  $\text{Ba}_2\text{Cu}_3\text{O}_4\text{Cl}_2$  are ZRS's. Here, we show ARPES spectra recorded at

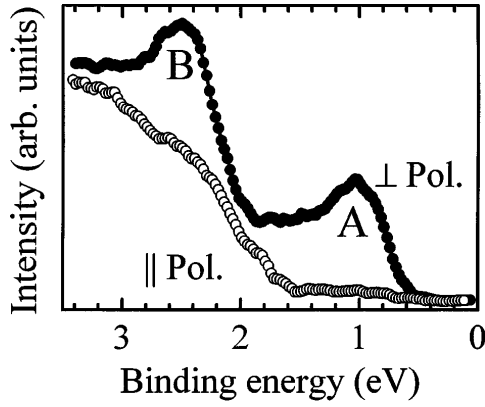


FIG. 3. Polarization-dependent ARPES spectra of  $\text{Ba}_2\text{Cu}_3\text{O}_4\text{Cl}_2$  at the  $(\pi, 0)$  point of the Brillouin zone measured with the electric field vector perpendicular ( $\bullet$ ) and parallel ( $\circ$ ) to the mirror plane  $M_1$ .

$(\pi, 0)$  with the polarization vector of the radiation aligned either parallel or perpendicular to the mirror plane  $M_1$  (see Fig. 1). Because of the experimental geometry used, this results in photoemission from initial states of either pure even (parallel) or odd (perpendicular) symmetry in regard to reflection in  $M_1$ . As can be seen from Fig. 3, the ZRS peak (and part of feature  $B$ ) disappears completely for the parallel case, thus attesting to the pure odd character of the initial state concerned. Further polarization-dependent measurements [9] show the same behavior for the lowest BE feature at  $\mathbf{k}$  values between  $(\pi, 0)$  and  $(3\pi, 0)$ . Upon consideration of the  $\text{Cu}_3\text{O}_4$  plane geometry shown in Fig. 1, it is apparent that a purely antibonding combination of the Cu  $3d_{x^2-y^2}$  and O  $2p_{x,y}$  orbitals yields a feasible initial state with the correct symmetry, whereas a nonbonding configuration, for example, would not. This is fully consistent with the ZRS character of the first electron removal states in  $\text{Ba}_2\text{Cu}_3\text{O}_4\text{Cl}_2$ .

Up to now, we have discussed the qualitative differences between the dispersion relation of ZRS's in the  $\text{Cu}_3\text{O}_4$  plane of  $\text{Ba}_2\text{Cu}_3\text{O}_4\text{Cl}_2$  and the  $\text{CuO}_2$  plane of  $\text{Sr}_2\text{CuO}_2\text{Cl}_2$ , and have suggested that the former indicates the presence of two different ZRS's. In order to explore this idea further, we have calculated the motion of these singlets using a model Hamiltonian containing the relevant orbitals and correlation at the copper sites only. The tight-binding parameters result from a fit to the band structure [10] for  $\text{Ba}_2\text{Cu}_3\text{O}_4\text{Cl}_2$  calculated using the method of linear combination of optimized atomic orbitals. The coupling between the two O  $2p$  orbital subsystems is provided by the small parameter  $t_{pp}^{\parallel} = 0.2$  eV [10], which can be neglected in a first analysis [11]. In analogy with  $\text{Sr}_2\text{CuO}_2\text{Cl}_2$ , the motion on the  $\text{Cu}_A$  sublattice can be described by a  $t$ - $J$  model [4], including additional hopping parameters to second and third neighbors [12]. The parameters of such an extended  $t$ - $J$  model can be derived from the  $\text{Cu}_A$  part of our model Hamiltonian by means of the cell-perturbation method [13]. An analogous reduc-

tion procedure was also performed for the  $\text{Cu}_B$  sublattice. Each  $\text{Cu}_B$   $3d_{x^2-y^2}$  hybridizes with a combination of O  $2p$  orbitals with  $b_1$  symmetry (shown shaded in Fig. 1), denoted here by  $\pi_{i\sigma} = (p_{1\sigma} - p_{2\sigma} - p_{3\sigma} + p_{4\sigma})_i/2$ . The Hamiltonian (in hole representation) reads

$$H = \varepsilon_d^B \sum_{i\sigma} d_{i\sigma}^\dagger d_{i\sigma} + U_d \sum_i n_{i\uparrow}^d n_{i\downarrow}^d + \varepsilon_p \sum_{i\sigma} \pi_{i\sigma}^\dagger \pi_{i\sigma} - \frac{t_{pp}^\perp}{2} \sum_{\langle ij \rangle} \pi_{i\sigma}^\dagger \pi_{j\sigma} + 2t_{pd} \sum_i (d_{i\sigma}^\dagger \pi_{i\sigma} + \text{H.c.}), \quad (1)$$

where the summations run over the  $\text{Cu}_B$  sublattice only and the parameters are  $t_{pp}^\perp = 0.45$  eV,  $t_{pd} = 1.7$  eV,  $\varepsilon_p - \varepsilon_d^B = 3.6$  eV, and  $U_d = 10.5$  eV [10,14]. In the cell-perturbation method, one diagonalizes (1) within a single cell consisting of one  $\text{Cu}_B$  and four oxygen atoms, and considers the coupling to neighboring cells as a perturbation. Adding a hole to the lowest one-hole state within one cell  $|\bar{d}\sigma\rangle = \cos\beta|d\sigma\rangle - \sin\beta|\pi\sigma\rangle$  creates predominantly the  $\text{ZRS}_B$  state  $|\Psi\rangle$  which is given by a linear combination of the three possible one-cell singlet states. The higher lying states are projected out, and the overlap between neighboring  $\text{ZRS}_B$ 's is provided by  $t_{pp}^\perp$ . The hopping of  $\text{ZRS}_B$ 's can be derived from the corresponding hopping term in (1):

$$-\frac{t_{pp}^\perp}{2} \pi_{i\sigma}^\dagger \pi_{j\sigma} \rightarrow t_B X_i^{\Psi, \bar{d}\sigma} X_j^{\bar{d}\sigma, \Psi}, \quad (2)$$

with  $t_B = -\eta^2 t_{pp}^\perp / 2$  and written in terms of Hubbard operators  $X_i^{\Psi, \bar{d}\sigma} = |\Psi_i\rangle \langle \bar{d}\sigma i|$ . The value of  $\eta = 0.75$  is calculated by diagonalizing the  $3 \times 3$  matrix of the two-hole singlet states within one cell which results in  $t_B = -0.13$  eV.

To calculate the dispersion of one hole in the two independent  $t$ - $J$  models, one has to take into account the corresponding magnetic background. As pointed out above, this reveals an important difference between  $\text{Cu}_A$  and  $\text{Cu}_B$ . The experiment was performed at  $T = 360$  K, which is much larger than  $T_N^B$  but of the order of  $T_N^A$ . Therefore, we may assume that while the magnetic correlation length on the  $\text{Cu}_A$  sublattice is much larger than the size of the magnetic polaron, its value on the  $\text{Cu}_B$  sublattice can be expected to be of the order of the  $\text{Cu}_B$  sublattice spacing. Correspondingly, the  $\text{ZRS}_B$  moves in a paramagnetic background, where its dispersion is determined by the nearest neighbor hopping,

$$E_k^{(B)} = E_0^{(B)} + t_B (\cos k_x a + \cos k_y a), \quad (3)$$

with a reduction of the bandwidth by only a factor of 2 [15] in comparison with free fermions, and where a strong broadening from thermal fluctuations can be expected. However, the  $\text{ZRS}_A$  moves in an antiferromagnetic background, where nearest neighbor hopping (with

respect to  $\text{Cu}_A$ ) is suppressed and where the dispersion is well known [4]:

$$E_k^{(A)} = E_0^{(A)} + 0.55J_A(\cos k_S + \cos k_D)^2 + \lambda(\cos k_S - \cos k_D)^2, \quad (4)$$

where  $k_{S/D} = a(k_x \pm k_y)/2$  is the transformation to the BZ of  $\text{Ba}_2\text{Cu}_3\text{O}_4\text{Cl}_2$ . The bandwidth of (4) is  $2.2J_A$  [4], with the parameter  $\lambda = 0.1$  eV describing the influence of the additional hopping parameters [12]. The energy difference  $E_0^{(B)} - E_0^{(A)}$  is determined by the local orbital energies and the binding energies of both the ZRS's and the magnetic polaron on the  $\text{Cu}_A$  sublattice. Its value was estimated to be roughly 0.5 eV.

In Fig. 4, we plot the experimental  $E(\mathbf{k})$  dispersion relation of the ZRS's in the  $\text{Cu}_3\text{O}_4$  plane. The width of the symbols represents the experimental  $\mathbf{k}$  resolution, and the height of the error bars represents the uncertainty in pinpointing the energy position of the feature concerned (showing, for example, that around the  $\Gamma$  point the exact energy position of the ZRS's is difficult to define). The dispersion relations of the  $\text{ZRS}_A$  and  $\text{ZRS}_B$  from (3) and (4) are shown as the dotted and solid lines in Fig. 4. It is clear that the experimentally observed dispersion can be well described without exceeding the limits of the parameters' theoretical estimation. In particular, the dispersion of  $\text{ZRS}_B$  between  $(\pi, 0)$  and  $(3\pi, 0)$  is reproduced, as is the presence of the  $\text{ZRS}_B$  as an "extra" feature at higher BE's, seen experimentally near  $(3\pi, 0)$ . The overall ZRS bandwidth is hard to determine exactly, thus, using Eq. (4),

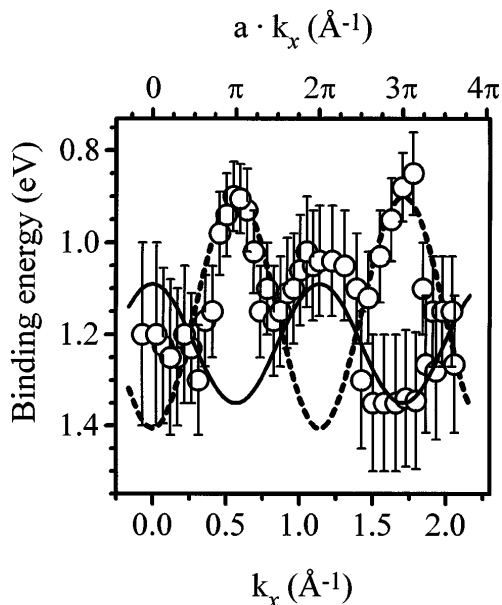


FIG. 4. Experimental dispersion relation of the Zhang-Rice singlets along  $(k_x, 0)$  (symbols), compared with a superposition of the calculated dispersions (3) ( $\text{ZRS}_B$ , solid line) and (4) ( $\text{ZRS}_A$ , dotted line). For the parameters used in the calculation, see the text.

only a rough estimate of  $J_A = (230 \pm 60)$  meV can be made, which is somewhat larger than both the value derived in Ref. [7] and the usual values for  $\text{CuO}_2$  cuprate planes.

In summary, ARPES spectra of  $\text{Ba}_2\text{Cu}_3\text{O}_4\text{Cl}_2$  indicate the presence of two Zhang-Rice singlets in the  $\text{Cu}_3\text{O}_4$  plane. The first belongs to the  $\text{Cu}_A\text{O}_2$  subsystem, whose antiferromagnetic ordering results in a dispersion proportional to the exchange integral,  $J_A$ , in analogy with observations of the paradigm  $\text{CuO}_2$  plane antiferromagnet  $\text{Sr}_2\text{CuO}_2\text{Cl}_2$ . The second stems from the  $\text{Cu}_B$  subsystem, and our model calculations show that its dispersion is consistent with that of a hole moving in a *paramagnetic* background—the bandwidth being proportional to the hopping integral between  $\text{Cu}_B$  sites,  $t_B$ . Thus, with regard to the dispersion of a hole in a magnetic spin background, the  $\text{Cu}_3\text{O}_4$  plane of  $\text{Ba}_2\text{Cu}_3\text{O}_4\text{Cl}_2$  represents simultaneously both the low and very high doping limits in cuprate materials.

This work was funded by the BMBF (Project No. 05-605BDA) and "Fonds der chemischen Industrie" (G.K.). M.S.G. is grateful to the EU for funding under the HCM Programme, and S.H. and H.R. to the DFG for support via the "Graduiertenkolleg der TU-Dresden." We thank S.-L. Drechsler and J. Schulenburg for useful discussions, and W. Höppner for her help in the preparation of the single crystals.

\*Permanent address: Joint Institute for Nuclear Research, 141980 Dubna, Russia.

- [1] F. C. Zhang and T. M. Rice, Phys. Rev. B **37**, 3759 (1988).
- [2] B. O. Wells *et al.*, Phys. Rev. Lett. **74**, 964 (1995).
- [3] J. J. M. Pothuisen, *et al.*, Phys. Rev. Lett. **78**, 717 (1997).
- [4] See, for example, E. Dagotto, Rev. Mod. Phys. **66**, 763 (1994), and references therein.
- [5] K. Yamada, N. Suzuki, and J. Akimitsu, Physica (Amsterdam) **213B-214B**, 191 (1995).
- [6] R. Kipka and Hk. Müller-Buschbaum, Z. Anorg. Allg. Chem. **419**, 58 (1976).
- [7] F. C. Chou *et al.*, Phys. Rev. Lett. **78**, 535 (1997).
- [8] W. B. Peatmann *et al.*, Rev. Sci. Instrum. **66**, 2801 (1995).
- [9] H. C. Schmelz *et al.* (unpublished).
- [10] H. Rosner and R. Hayn, Physica (Amsterdam) (to be published).
- [11] In Ref. [7], a very slight anisotropic coupling of the  $\text{Cu}_A$  and  $\text{Cu}_B$  systems is responsible for the ferromagnetic moment of  $\text{Sr}_2\text{Cu}_3\text{O}_4\text{Cl}_2$  at temperatures below  $T_N^A$ .
- [12] A. Nazarenko *et al.*, Phys. Rev. B **51**, 8676 (1995); J. Bala, A. Oleś, and J. Zaanen, Phys. Rev. B **52**, 4597 (1995).
- [13] L. F. Feiner, J. H. Jefferson, and R. Raimondi, Phys. Rev. B **53**, 8751 (1996); V. I. Belinicher, A. L. Chernyshev, and V. A. Shubin, Phys. Rev. B **53**, 335 (1996); V. Yu. Yushankhai, V. S. Oudovenko, and R. Hayn, Phys. Rev. B (to be published).
- [14] M. S. Hybertsen *et al.*, Phys. Rev. B **41**, 11 068 (1990).
- [15] R. Hayn, V. Yushankhai, and S. Lovtsov, Phys. Rev. B **47**, 5253 (1993).